

Ultrafast electron dynamics in platinum and gold thin films driven by optical and terahertz fields

Cite as: Appl. Phys. Lett. **120**, 021601 (2022); <https://doi.org/10.1063/5.0068086>

Submitted: 23 August 2021 • Accepted: 26 November 2021 • Published Online: 10 January 2022

Published open access through an agreement with Stockholm Universitet

V. Unikandanunni, F. Rigoni,  M. C. Hoffmann, et al.

COLLECTIONS

 This paper was selected as Featured



View Online



Export Citation



CrossMark

ARTICLES YOU MAY BE INTERESTED IN

[Quantum technologies in diamond enabled by laser processing](#)

Applied Physics Letters **120**, 020502 (2022); <https://doi.org/10.1063/5.0080348>

[A perspective on elastic metastructures for energy harvesting](#)

Applied Physics Letters **120**, 020501 (2022); <https://doi.org/10.1063/5.0078740>

[Atomically thin gallium telluride nanosheets: A new 2D material for efficient broadband nonlinear optical devices](#)

Applied Physics Letters **120**, 021101 (2022); <https://doi.org/10.1063/5.0073205>

Lock-in Amplifiers
up to 600 MHz



Zurich
Instruments



Ultrafast electron dynamics in platinum and gold thin films driven by optical and terahertz fields

Cite as: Appl. Phys. Lett. **120**, 021601 (2022); doi: [10.1063/5.0068086](https://doi.org/10.1063/5.0068086)

Submitted: 23 August 2021 · Accepted: 26 November 2021 ·

Published Online: 10 January 2022



View Online



Export Citation



CrossMark

V. Unikandanunni,¹ F. Rigoni,² M. C. Hoffmann,³  P. Vavassori,⁴  S. Urazhdin,⁵ and S. Bonetti^{1,2,a)} 

AFFILIATIONS

¹Department of Physics, Stockholm University, SE-10691 Stockholm, Sweden

²Department of Molecular Sciences and Nanosystems, Ca' Foscari University of Venice, 30172 Venice, Italy

³Linear Coherent Light Source, SLAC National Accelerator Laboratory, Menlo Park, California 94025, USA

⁴CIC nanoGUNE BRTA, San Sebastian, Spain and IKERBASQUE, Basque Foundation for Science, Bilbao, Spain

⁵Department of Physics, Emory University, Atlanta, Georgia 30322, USA

^{a)} Author to whom correspondence should be addressed: stefano.bonetti@fysik.su.se

ABSTRACT

We investigate the ultrafast electron dynamics triggered by terahertz and optical pulses in thin platinum and gold films by probing their transient optical reflectivity. The response of the platinum film to an intense terahertz pulse is similar to the optically induced one and can be described by a two-temperature model with a 20% larger electron–phonon coupling for the terahertz-driven dynamics compared to the optically induced one, ascribed to an additional nonthermal electron–phonon coupling contribution. Surprisingly, gold films exhibit a much smaller terahertz pulse-induced reflectivity change and with a sign opposite to the optical case. We explain this remarkable observation with field emission of electrons due to Fowler–Nordheim tunneling, enabled in samples with thicknesses below the structural percolation threshold, where nanostructuring promotes near-field enhancement. Our results provide a fundamental insight into the ultrafast processes relevant to modern electro- and magneto-optical applications.

© 2022 Author(s). All article content, except where otherwise noted, is licensed under a Creative Commons Attribution (CC BY) license (<http://creativecommons.org/licenses/by/4.0/>). <https://doi.org/10.1063/5.0068086>

The advent of intense single-cycle terahertz (THz) radiation sources has opened new avenues for the exploration of the light–matter interaction with accessible electric fields of the order of MV/cm at photon energies in the meV range. With the emergence of these sources, it is now possible to study the THz-driven ultrafast dynamics of coupled degrees of freedom in condensed matter systems.^{1–5} Efforts under way are aiming, using near-field enhancement in metamaterials,⁶ to reach local electric field strengths of the order of 100 MV/cm (1 V/Å), comparable to that of the interatomic fields. Metals provide an excellent medium to investigate THz-induced coupled many-body dynamics, thanks to the presence of multiple degrees of freedom able to interact with THz radiation, including free electrons, phonons, and magnons in magnetic materials. A variety of THz-driven physical processes ranging from ultrafast demagnetization in magnetic thin films⁷ to field emission in nanotips have been recently reported in the literature,⁸ which were earlier observed only in the optical regime.^{9,10} Hence, one can now perform ultrafast studies with electromagnetic pulses with comparable intensity but in two regions of the electromagnetic spectrum that differ in frequency by three orders of magnitude.

This is expected to provide unprecedented insight into the fundamental understanding of the light–matter interaction.^{11,12}

Optically induced ultrafast dynamics in metals is usually discussed using a phenomenological two-temperature model (2TM).¹³ This model is, in principle, applicable to dynamics driven by THz radiation as well, since it does not rely on the specific mechanism of excitation but only on the total energy deposited by radiation into the material. According to the 2TM, ultrafast pulses directly excite energetic electrons, which, within tens of femtoseconds, thermalize via electron–electron collisions to a Fermi–Dirac distribution at a higher temperature. Only at later times (hundreds of femtoseconds), they thermalize with the lattice. However, time-resolved photoemission spectroscopy measurements have shown that the 2TM assumption of distinct time scales is not always valid, and the nonequilibrium electron population can exist for up to 1 ps in materials such as gold.^{14,15} No data exist for the case of THz-driven excitations. Even more fundamental approaches, such as the one offered by the Fermi liquid theory, which correctly describe eV excitations with the characteristic $\tau^{-1} \sim (E - E_F)^2$ dependence, break down when the photon energy is

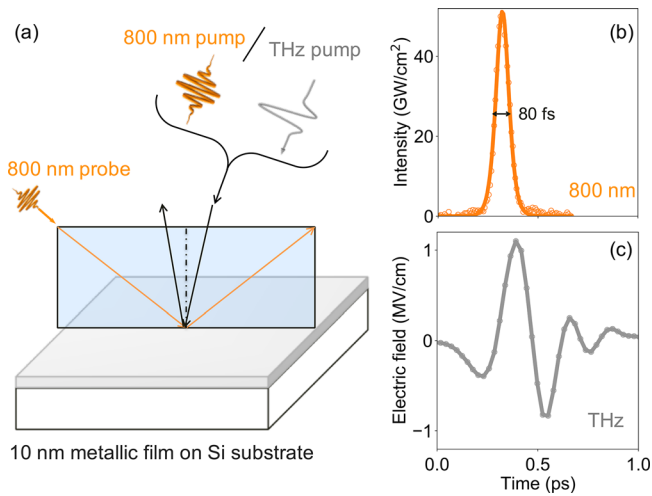


FIG. 1. (a) Geometry of the experimental setup to measure the transient reflectivity. The plane of incidence is marked in blue. (b) Autocorrelator trace of the 800 nm pump intensity. (c) Temporal profile of the electric field of the THz pulse. The symbols in panels (b) and (c) are the measured data. The solid line in panel (b) is the best fit obtained with a Gaussian function, and the line in panel (c) is a guide to the eye.

lowered toward the meV range.^{16,17} In fact, in this energy range, more correct models of ultrafast electron dynamics must also include a temperature dependent term, which prevents an indefinite slowdown of the relaxation with lowering photon energy.¹⁸

In this Letter, we compare the dynamics induced by THz and near-infrared radiation in 10-nm-thick platinum and gold films, two metals that are neighbors in the periodic table with very different band

structures. Both materials are of broad current interest in condensed matter physics.^{19–21} Platinum is widely used in magnetic and magneto-optical experiments and is a key material in spintronics due to its large spin–orbit coupling. Gold is essential in plasmonics and for the fabrication of metamaterials, thanks to its low Ohmic losses.^{22–24} By performing time-resolved reflectivity measurements using 800 nm probe pulses and by simulating the dynamics using a 2TM, we gain a detailed understanding of the dynamics at play, which we expect to be relevant for other metals with similar electronic configuration.

The 800 nm pump–probe experiments are performed with the pump derived from the fundamental of an amplified Ti:sapphire laser with the geometry sketched in Fig. 1(a). The temporal profile of the pump pulse intensity measured using an autocorrelator is shown in Fig. 1(b). The THz pump–optical probe experiments are conducted with the THz field with a peak amplitude of approximately 1 MV/cm, as shown in Fig. 1(c), where the electro-optical sampling signal of a 50 μm thick GaP crystal is shown.²⁵ The incident fluence is around 2.5 mJ/cm^2 for both THz and 800 nm pumps. The change in reflectivity of the 800 nm probe is measured using a silicon photo-detector. Further details of the setup are given in the [supplementary material](#).

Figures 2(a) and 2(b) show the transient reflectivity in platinum and, respectively, gold. For both materials, the reflectivity change caused by the THz (800 nm) pump is shown by gray (orange) symbols. The continuous lines in Figs. 2(c) and 2(d) show the 2TM simulation results. The calculated absorbance of both pumps as a function of the sample depth is given in the insets. Both calculations are based on the transfer matrix method, implemented using the open-source simulation package NTMpy.²⁶ The material parameters and other simulation details are provided in the [supplementary material](#).

We first discuss the results for platinum in Fig. 2(a). The transient reflectivity shows a qualitatively similar response for both THz

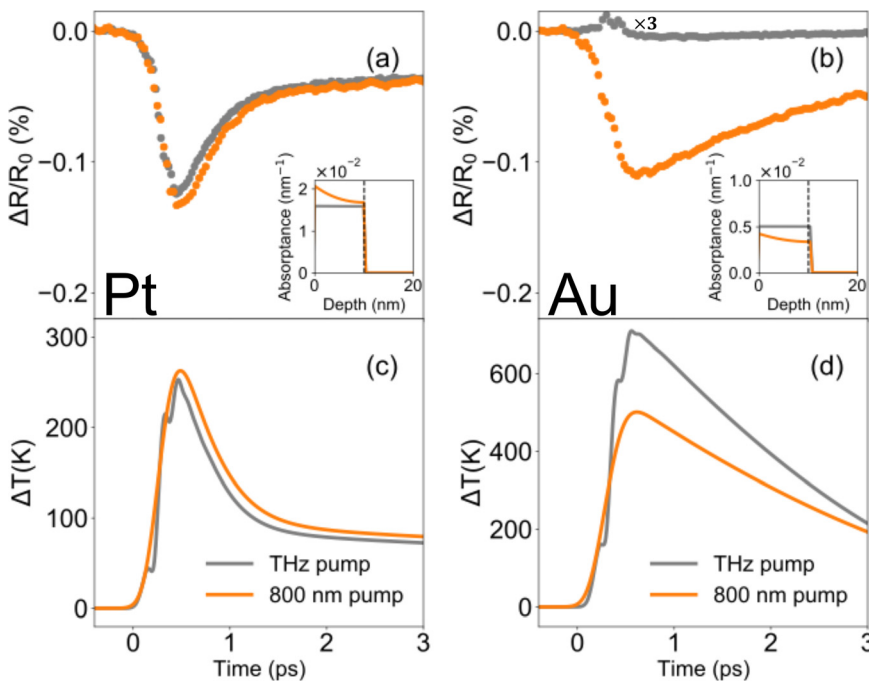


FIG. 2. Symbols: transient reflectivity of (a) platinum and (b) gold samples after excitation with THz (gray) and 800 nm (orange) pump pulses. The solid lines in panels (c) and (d) show the temperature evolution in platinum and gold calculated using the 2TM detailed in the main text. Insets: simulated absorbance profile for the two pump wavelengths.

TABLE I. Electron–phonon coupling G extracted from the data in Fig. 2 using 2TM simulation and the corresponding values from the literature. In Ref. 27, the pump wavelength used was 400 nm, and in Ref. 28, it was in the range 780–880 nm, while Refs. 29 and 30 are theoretical works where a wavelength-independent G is computed.

	G_{THz} (W/m ³ K)	G_{800} (W/m ³ K)	G^{27-30} (W/m ³ K)
Platinum	$(11.2 \pm 0.1) \times 10^{17}$	$(9.3 \pm 0.1) \times 10^{17}$	$(2.5-11) \times 10^{17}$
Gold	...	$(2.2 \pm 0.1) \times 10^{16}$	$(2.1 \pm 0.3) \times 10^{16}$

pump and 800 nm pump with a maximum relative change reaching approximately 0.1% after less than 1 ps. After that, the reflectivity rapidly relaxes to 0.05% after a couple of picoseconds, followed by a slow recovery toward equilibrium at much longer times. The absorbed fluence is similar for the two different pump energies, and it leads to a maximum temperature change of approximately 250 K according to 2TM simulations. These simulations capture the time dependent optical response, allowing us to extract the electron–phonon coupling G for the two cases, as shown in the first row of Table I. The electron–phonon coupling extracted for the THz-induced dynamics $G_{\text{THz}}^{\text{Pt}}$ is about 20% larger than the one for optical frequencies G_{800}^{Pt} . This is a relevant finding, since G is usually assumed to be independent of the pump wavelength in the optical region.

Moving to the gold response in Fig. 2(b), we note that for the 800 nm pump, the initial transient decrease in reflectivity also occurs within less than 1 ps and reaches a similar maximum relative variation of 0.1% comparable to the response of platinum. The subsequent recovery toward equilibrium is, on the other hand, much slower than for platinum; the electron–phonon coupling extracted from these data using 2TM simulations is indeed 50 times smaller. The same model returns a maximum temperature increase of approximately 450 K. Aside from these quantitative differences, the transient reflectivity with the 800 nm pump is qualitatively similar for the two metals. On the contrary, the reflectivity change in gold driven by the THz pump, shown by the gray symbols, is much different: it is more than an order of magnitude smaller in amplitude, and opposite in sign, i.e., it is a positive variation rather than a negative one. Before going into a detailed explanation, we point out that the size of the effect is not a trivial effect due to a smaller pump absorption. The inset of Fig. 2(b) shows, in fact, that the expected absorbance of THz radiation would be even slightly larger for THz than that for the 800 nm light. Hence, a different mechanism must be in place when intense THz fields are

used, and which, crucially, also needs to explain the increase in the transient reflectivity.

To gain insight into all the data presented so far, we plot in Figs. 3(a) and 3(b) the electronic and the phonon density of states (DOS) for the two materials. The orange and gray shadings, respectively, represent the initial bandwidth of the nonthermal electrons excited by the 800 nm pump and the THz pump. The 800 nm pump excites electrons up to 1.55 eV away from the Fermi level, whereas the THz pump up to a maximum of 30 meV. It is known that electron scattering occurring in proximity of the Fermi level contributes the most to the electron–phonon coupling.^{33,34} For the 800 nm excitation, the majority of the nonthermal electrons are far from the Fermi level, so the contribution of electron–phonon coupling to their relaxation is initially negligible and becomes effective only after they thermalize.¹⁵

First, we apply these general observations to the case of platinum, where the two excitations give rise to similar dynamics. The material has a comparatively large number of available electronic states with localized d character around the Fermi level. This electronic configuration leads to a relatively large density of excited electrons, which, in turn, enhances the scattering with phonons for both 800 nm and THz induced dynamics. For the case of terahertz fields, the characteristic energy of the excited electrons is lower than for the 800 nm one, requiring fewer electron–electron scattering events to thermalize to the Fermi energy. Consequently, the contribution of electron–phonon scattering is larger,^{7,12} explaining the observed $G_{\text{THz}}^{\text{Pt}} > G_{800}^{\text{Pt}}$.

For the case of gold, the situation is remarkably different. The phonon DOS is similar to that of platinum. However, the electronic DOS is substantially different. In particular, the density of states within about 1 eV from the Fermi level is dominated by itinerant s -states with a negligible contribution from the localized d -states and, importantly, a much reduced density of available states. These two facts result in a much weaker electron–phonon coupling, consistent with the observed

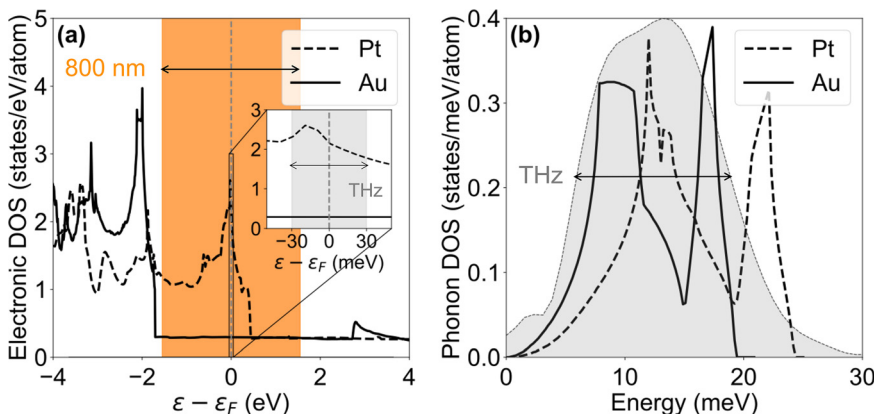


FIG. 3. (a) Electronic and (b) phonon density of states (DOS) for platinum (dashed lines) and gold (solid lines). The calculated DOS are taken from Refs. 29, 31, and 32. The orange and gray shading illustrate the maximum bandwidth of the nonthermal electrons excited by the 800 nm and THz pumps, respectively. Inset in panel (a): magnification of the main panel, showing the density of states for the two materials close to the Fermi level.

$G_{800}^{\text{Au}} \ll G_{800}^{\text{Pt}}$ (see Table I). However, this observation by itself does not provide an explanation for neither the much weaker THz-induced reflectivity change nor its opposite sign compared to the 800 nm pump, which is the most striking result in Fig. 2 and in clear contrast with the 2TM calculations. We note, in particular, that for thermalized electrons, a THz-induced increase in the transient reflectivity would imply a decrease in temperature in an apparent violation of the conservation of energy. 2TM simulations predict for gold a comparable electronic temperature change for both optical and THz pumps [Fig. 2(b)], confirming the breakdown of the model, and suggesting that a mechanism other than thermalization must also be at play.

We argue that our observations relate to the emission from the gold film of electrons accelerated by the strong THz electric field. Qualitatively, this mechanism is understood assuming that the THz field tilts the potential barrier, in turn enabling electron tunneling into the vacuum without sample heating. Electron emission has already been observed in nano-tips and metallic metasurfaces made of gold, tungsten, and other materials,^{8,35,36} where the near-field enhancement helps reaching the threshold of emission. More recently, THz-driven electron emission was observed from a gold surface using a peak electric field as low as 50 kV/cm without any local enhancement, although the thickness and other characteristics of the sample were not reported.^{37,38} The observation of field emission in ultrathin gold films deposited on a solid substrate is, however, still missing, a geometry that is the most relevant for many applications. Field-induced electron emission is explained by the Fowler–Nordheim model of quantum mechanical tunneling.³⁹ The probability of field emission for THz electric fields of frequency f and peak amplitude E_{THz} is related to the value of Keldysh parameter⁴⁰ $\gamma_k = 2\pi f \sqrt{2m\phi} / eE_{\text{THz}}$, where ϕ , m , and e are the work function, the mass, and the charge of the electron, respectively. Field emission is dominant for $\gamma_k \ll 1$, whereas photoionization dominates for $\gamma_k \gg 1$. For our experimental parameters and $\phi = 5.2$ eV, $\gamma_k \approx 1.2$. When $\gamma_k \approx 1$, the dominant physical effect is less obvious. Uiberacker and coworkers⁴¹ have reported field emission for a value of Keldysh parameter as high as three.

To further test our hypothesis, in Fig. 4 we zoom in on the initial transient response to the THz field of the evaporated gold film described thus far, together with the response of a sputtered gold film. By overlaying the square of the measured THz electric field E_{THz} on the evaporated gold data, it is clear that the time profile of the initial transient reflectivity goes as E_{THz}^2 . Since the Fowler–Nordheim tunneling current is also proportional to E_{THz}^2 ,³⁹ this further supports the argument that the THz induced transient reflectivity in evaporated gold is dominated by electron field emission. The sign of the effect, i.e., the transient increase in the reflectivity in the first 500 fs, is expected when the plasma frequency decreases. This is, in turn, compatible with a Drude–Lorentz picture when the electron density reduces, as it would be the case when electron field emission occurs. The rather laborious algebraic derivation is presented in the supplementary material.

In addition, we also observe a rectification behavior, modeled with a Gaussian-like shape mimicking the terahertz field carrier envelope. Such behavior flips its sign when we change the polarization of the THz pump pulse by 180°, as shown in the inset of Fig. 4. This rectification effect is thought as the net normal component of the THz electric field arising due to the slight asymmetry of the film interfaces (air/gold and gold/substrate). The subsequent decrease in reflectivity at later times is understood as the thermalization of electrons with the

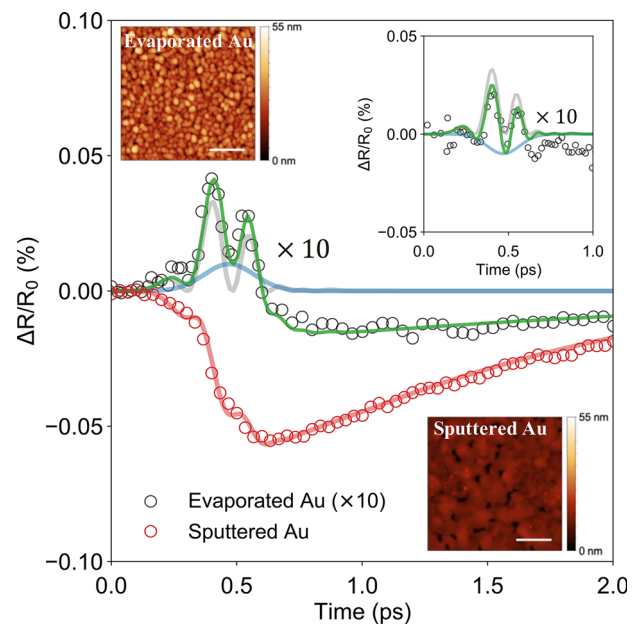


FIG. 4. Symbols: Experimental transient reflectivity of gold in the first 2 ps excited by the terahertz field E_{THz} . Gray solid line: E_{THz}^2 , with E_{THz} measured independently using electro-optic sampling in a GaP crystal. Blue solid line: THz field rectification modeled as a scaled Gaussian envelope of E_{THz} . Green solid line: fit of the data including adding up E_{THz}^2 , rectification signal, and an exponential recovery. Inset: same as the main panel but with the THz pump field polarity reversed by 180°. Images: AFM scans of the evaporated (top) and sputtered (bottom) gold films. The scale bar is 500 nm for both films.

lattice, observed in all other samples as well. However, the effect is now significantly reduced, since most of the energy from radiation has already been transferred into kinetic energy of the emitted electrons that have left the sample. A good fit to the data is obtained when the three effects: electron field emission, rectification, and thermalization are considered. Crucially, we notice that all these effects are gone, and the conventional 2TM behavior is recovered in the sputtered film, where we also find a 30% larger G value as compared to 800 nm radiation, similarly to what observed in the case of platinum.

The 2TM-like behavior in the sputtered gold film with much lower roughness than the evaporated one, clearly shown by the atomic force microscopy (AFM) images in Fig. 4, suggests that the microscopic structure of the gold film plays a key role. It has been reported that nm-scale inhomogeneity in metals leads to near-field enhancement of electric fields^{42,43} and that metamaterials comprising nm gaps work effectively in enhancing THz fields.⁴⁴ A larger local THz electric field lowers γ_k further into the field emission regime. We stress that selfnanostructuring is a well-known property of thin gold films below a critical thickness of the order of 10 nm, not a sign of lower quality samples. The films are homogeneous at spatial scales comparable with the wavelength of visible and terahertz light. In fact, the transient reflectivity induced by 800 nm light in Fig. 2(b) shows the expected response for gold. We show in the supplementary material that a thicker gold film (50 nm, above the percolation threshold) deposited by evaporation shows no measurable field emission nor negative transient reflectivity.

Finally, the field emission probability decreases also with the character of the accelerated electrons. Theoretically, the tunneling probability for d -electrons is approximately three orders of magnitude lower than that of s -electron with the same energy.⁴⁵ This is due to the larger scattering cross section of d -electrons, which prevents them from being accelerated at large enough energies, and instead to first scatter and thermalize with the lattice. Pt has a relatively large density of d -states around the Fermi level, as shown in Fig. 3(a), and hence, electron field emission is expected to be much reduced in this material, even in the presence of nanostructuring.

In summary, we studied the THz and 800 nm induced electron and lattice dynamics in gold and platinum thin films measuring their transient optical reflectivity. Platinum showed a comparable response to both THz and optical pumps with 2TM simulations returning a 20% larger electron-phonon coupling G , when the material is excited by terahertz fields rather than with optical ones. We explain this evidence introducing an additional coupling channel only available when nonthermal electrons are excited close to the Fermi level. Hence, the common assumption of wavelength-independent G is not correct when pump wavelengths differing by orders of magnitude are considered. In gold, we found that the 2TM breaks down when nanostructured films are excited with intense terahertz fields. We propose that electronic field emission within the Fowler-Nordheim model can explain the experimental observations. We anticipate that our results will be highly relevant for many ultrafast experiments in magnetism and optics, where platinum, gold, or any metallic thin films with similar properties are incorporated as a part of heterostructures or in metamaterials.

See the [supplementary material](#) for (i) pump-probe setup details, (ii) two-temperature model simulations, (iii) sample characterization using THz time-domain spectroscopy, (iv) derivation of the relationship between transient optical reflectivity and material properties, (v) THz transient reflectivity in 50 nm films, and (vi) atomic force microscopy measurements.

V.U. and S.B. acknowledge support from the European Research Council, Starting Grant No. 715452 “MAGNETIC-SPEED-LIMIT,” and S.U. acknowledges support from the National Science Foundation via Award Nos. ECCS-1804198 and ECCS-2005786. P.V. acknowledges support from the Spanish Ministry of Economy, Industry, and Competitiveness under the Maria de Maeztu Units of Excellence Programme—No. CEX2020-001038-M.

AUTHOR DECLARATIONS

Conflict of Interest

The authors have no conflicts to disclose.

DATA AVAILABILITY

The data that support the findings of this study are available from the corresponding author upon reasonable request.

REFERENCES

- C. Ruchert, C. Vicario, and C. P. Hauri, *Opt. Lett.* **37**, 899 (2012).
- M. Liu, H. Y. Hwang, H. Tao, A. C. Strikwerda, K. Fan, G. R. Keiser, A. J. Sternbach, K. G. West, S. Kittiwatanakul, J. Lu *et al.*, *Nature* **487**, 345 (2012).
- T. Kampfrath, K. Tanaka, and K. A. Nelson, *Nat. Photonics* **7**, 680 (2013).
- C. Vicario, B. Monoszalai, and C. P. Hauri, *Phys. Rev. Lett.* **112**, 213901 (2014).
- H. Hafez, X. Chai, A. Ibrahim, S. Mondal, D. Férachou, X. Ropagnol, and T. Ozaki, *J. Opt.* **18**, 093004 (2016).
- P. Salén, M. Basini, S. Bonetti, J. Hebling, M. Krasilnikov, A. Y. Nikitin, G. Shamuilov, Z. Tibai, V. Zhaunerchyk, and V. Goryashko, *Phys. Rep.* **836–837**, 1–74 (2019).
- S. Bonetti, M. Hoffmann, M.-J. Sher, Z. Chen, S.-H. Yang, M. Samant, S. Parkin, and H. Dürr, *Phys. Rev. Lett.* **117**, 087205 (2016).
- S. Li and R. Jones, *Nat. Commun.* **7**(1), 13405 (2016).
- E. Beaufrepaire, J.-C. Merle, A. Daunois, and J.-Y. Bigot, *Phys. Rev. Lett.* **76**, 4250 (1996).
- G. Herink, D. R. Solli, M. Gulde, and C. Ropers, *Nature* **483**, 190 (2012).
- B. G. Alberding, G. P. Kushto, P. A. Lane, and E. J. Heilweil, *Appl. Phys. Lett.* **108**, 223104 (2016).
- A. Levchuk, B. Wilk, G. Vaudel, F. Labbé, B. Arnaud, K. Balin, J. Szade, P. Ruello, and V. Juvé, *Phys. Rev. B* **101**, 180102 (2020).
- S. Anisimov, B. Kapeliovich, T. Perelman *et al.*, *Zh. Eksp. Teor. Fiz.* **66**, 375 (1974).
- W. Fann, R. Storz, H. Tom, and J. Bokor, *Phys. Rev. Lett.* **68**, 2834 (1992).
- W. Fann, R. Storz, H. Tom, and J. Bokor, *Phys. Rev. B* **46**, 13592 (1992).
- D. Pines and P. Nozières, *The Theory of Quantum Liquids: Normal Fermi Liquids* (Benjamin, 1966), Vol. 1.
- D.-S. Kim, J. Shah, J. Cunningham, T. Damen, S. Schmitt-Rink, and W. Schäfer, *Phys. Rev. Lett.* **68**, 2838 (1992).
- R. H. Groeneveld, R. Sprik, and A. Lagendijk, *Phys. Rev. B* **51**, 11433 (1995).
- R. B. Wilson and S. Coh, *Commun. Phys.* **3**(1), 179 (2020).
- D. Zahn, H. Seiler, Y. W. Windsor, and R. Ernstorfer, [arXiv:2012.10428](#) (2020).
- K. Liu, X. Shi, R. Mohan, J. Gorchon, S. Coh, and R. B. Wilson, [arXiv:2103.06337](#) (2021).
- Y. Zhong, S. D. Malagari, T. Hamilton, and D. M. Wasserman, *J. Nanophotonics* **9**, 093791 (2015).
- W. T. Hsieh, P. C. Wu, J. B. Khurgin, D. P. Tsai, N. Liu, and G. Sun, *ACS Photonics* **5**, 2541 (2018).
- J. B. Khurgin, *Philos. Trans. R. Soc. A* **375**, 20160068 (2017).
- A. Nahata, D. H. Auston, T. F. Heinz, and C. Wu, *Appl. Phys. Lett.* **68**, 150 (1996).
- L. Alber, V. Scalera, V. Unikandanunni, D. Schick, and S. Bonetti, *Comput. Phys. Commun.* **265**, 107990 (2021).
- J. Hohlfeld, S.-S. Wellershoff, J. Güdde, U. Conrad, V. Jähnke, and E. Matthias, *Chem. Phys.* **251**, 237 (2000).
- A. P. Caffrey, P. E. Hopkins, J. M. Klopff, and P. M. Norris, *Microscale Thermophys. Eng.* **9**, 365 (2005).
- Z. Lin, L. V. Zhigilei, and V. Celli, *Phys. Rev. B* **77**, 075133 (2008).
- N. Smirnov, *Phys. Rev. B* **101**, 094103 (2020).
- H. Schober and P. Dederichs, in *Landolt Börnstein New Series*, Vol. 3 (Springer-Verlag, 1981), p. 130.
- A. Zhalko-Titarenko, V. Antonov, V. Nemoshkalenko, and W. John, *Phys. Status Solidi B* **132**, K15 (1985).
- V. Ginzburg and V. Shabanskii, *Dokl. Akad. Nauk SSSR* **100**, 445–448 (1955).
- M. Kaganov, E. Lifshitz, and L. Tanatarov, *Sov. Phys.-JETP* **4**, 173 (1957).
- T. L. Cocker, V. Jelic, M. Gupta, S. J. Molesky, J. A. Burgess, G. De Los Reyes, L. V. Titova, Y. Y. Tsui, M. R. Freeman, and F. A. Hegmann, *Nat. Photonics* **7**, 620 (2013).
- S. L. Lange, N. K. Noori, T. M. B. Kristensen, K. Steenberg, and P. U. Jepsen, *J. Appl. Phys.* **128**, 070901 (2020).
- C. Lombosi, I. Márton, Z. Ollmann, J. Hebling, G. Farkas, P. Dombi, and J. Fülöp, in *The European Conference on Lasers and Electro-Optics* (Optical Society of America, 2015), p. CC_3_1.
- S. Li, P. S. Nugraha, A. Sharma, C. Lombosi, Z. Ollmann, I. Márton, G. Farkas, J. Hebling, P. Dombi, and J. A. Fülöp, in *44th International Conference on Infrared, Millimeter, and Terahertz Waves (IRMMW-THz)* (IEEE, 2019).

- ³⁹R. H. Fowler and L. Nordheim, *Proc. R. Soc. London, Ser. A* **119**, 173 (1928).
- ⁴⁰L. Keldysh, *Sov. Phys. JETP* **20**, 1307 (1965).
- ⁴¹M. Uiberacker, T. Uphues, M. Schultze, A. J. Verhoef, V. Yakovlev, M. F. Kling, J. Rauschenberger, N. M. Kabachnik, H. Schröder, M. Lezius *et al.*, *Nature* **446**, 627 (2007).
- ⁴²V. Choukrov, in *XXIst International Symposium on Discharges and Electrical Insulation in Vacuum (ISDEIV)* (IEEE, 2004), Vol. 1, pp. 17–20.
- ⁴³K. Iwaszczuk, M. Zalkovskij, A. C. Strikwerda, and P. U. Jepsen, *Optica* **2**, 116 (2015).
- ⁴⁴J.-H. Kang, D.-S. Kim, and M. Seo, *Nanophotonics* **7**, 763 (2018).
- ⁴⁵J. Gadzuk, *Phys. Rev.* **182**, 416 (1969).